

Nonvolatile Multilevel Resistive Switching in Ar⁺ Irradiated BiFeO₃ Thin Films

Y. Shuai, X. Ou, W. Luo, N. Du, C. Wu, W. Zhang, D. Bürger, C. Mayr, R. Schüffny, S. Zhou, M. Helm, and H. Schmidt

Abstract—Low-energy Ar⁺ ion irradiation has been applied to an Au/BiFeO₃/Pt capacitor structure before deposition of the Au top electrode. The irradiated thin film exhibits multilevel resistive switching (RS) without detrimental resistance degradation, which makes the intermediate resistance states more distinguishable, as compared with the nonirradiated thin film. The stabilization of resistance states after irradiation is discussed based on the analysis of the conduction mechanism during the RS, which was investigated by means of temperature-dependent current–voltage measurement from room temperature to 423 K.

Index Terms—Irradiation, rectifying, resistive switching (RS).

I. INTRODUCTION

RESISTIVE switching (RS) has been widely studied in recent years due to the potential applications in next-generation nonvolatile memory devices [1], [2]. Bistable RS is usually observed in a metal–oxide–metal capacitor structure and has been shown to depend on the insulating or semiconducting oxide material [3], on the electrode material [4], and on the metal–oxide interface [5]. Aside from the bistable RS, multilevel RS has been also reported [6]. By adjusting the amplitude or the duration of the external voltage pulse, intermediate resistance states between the high- and low-resistance states (HRS and LRS, respectively) can be set. Nonvolatile multilevel switching can significantly increase the memory density without enlarging the device size [7]. However, if those intermediate resistance states are not stable enough, misreading occurs because adjacent resistance states remain indistinguishable. Therefore, long-term retention without obvious resistance degradation is needed in every intermediate resistance state.

As one of the most promising multiferroic materials, BiFeO₃ (BFO) shows RS. We have reported an interface-related bistable

Manuscript received October 16, 2012; revised November 6, 2012; accepted November 7, 2012. Date of publication December 13, 2012; date of current version December 19, 2012. This work was supported in part by the Deutsche Forschungsgemeinschaft under Grant SCHM1663/4 and in part by the Helmholtz-Gemeinschaft deutscher Forschungszentren under Grant VH-VI-442 and Grant VH-NG-713. The review of this letter was arranged by Editor T. Wang.

Y. Shuai, W. Luo, C. Wu, and W. Zhang are with State Key Laboratory of Electronic Thin Films and Integrated Devices, University of Electronic Science and Technology of China, 610054 Chengdu, China.

X. Ou, D. Bürger, S. Zhou, and M. Helm are with the Helmholtz-Zentrum Dresden-Rossendorf, 01314 Dresden, Germany (e-mail: X.Ou@hzdr.de).

N. Du and H. Schmidt are with Technische Universität Chemnitz, 09126 Chemnitz, Germany.

C. Mayr and R. Schüffny are with the Chair of Highly-Parallel VLSI-Systems and Neuromorphic Circuits, Technische Universität Dresden, 01069 Dresden, Germany.

Color versions of one or more of the figures in this letter are available online at <http://ieeexplore.ieee.org>.

Digital Object Identifier 10.1109/LED.2012.2227666

RS in an Au/BFO/Pt capacitor structure [8]. This type of RS does not need any electroforming process. The homogeneous conduction facilitates the downscaling of the RS device. However, it suffers from the resistance degradation [9]; thus, the correspondingly defined LRSs for multilevel RS cannot be regarded as nonvolatile anymore [7]. It is known that defects play an important role in RS and that intentional manipulation of defects, e.g., oxygen vacancies (OVs), can tailor RS behavior. Low-energy ion irradiation is a useful tool to tune the electrical properties of functional oxides by manipulating the OV distribution and concentration in oxides [10]. In this letter, we show that after Ar⁺ ion irradiation, multilevel RS without obvious degradation was obtained. To understand the stabilization of these multilevel resistance states, the conduction mechanisms of the BFO thin films before and after Ar⁺ ion irradiation were analyzed by means of temperature-dependent current–voltage (*I*–*V*) measurements.

II. EXPERIMENTS

BFO thin films were deposited by pulsed laser deposition on Pt/Ti/SiO₂/Si substrates. More details about the deposition parameters can be found in our previous report [8]. After deposition, irradiation with Ar⁺ ions was performed with a Kaufman ion source. An Ar⁺ beam with an energy of 300 eV, an ion flux of $6 \times 10^{14} \text{ cm}^{-2} \cdot \text{s}^{-1}$, and an ion fluence of $5 \times 10^{17} \text{ cm}^{-2}$ was applied in the irradiation process. Note that, under this Ar⁺ ion fluence, the irradiated sample has the largest ON/OFF current ratio. The thin-film thickness was reduced from 500 to 400 nm by the irradiation, which was measured by a surface profilometer (Dektak8, Veeco).

The Au layer was sputtered on the surface of the BFO thin films using a metal shadow mask. The electrical measurements were carried out with a Keithley 2400 source meter. The sample temperature (up to 423 K) was adjusted via a heating plate, and the surface temperature of the samples was monitored by a thermal element with an accuracy of ± 2.5 K.

III. RESULTS AND DISCUSSION

I–*V* curves measured at room temperature (RT) are shown in Fig. 1(a) and (c) for nonirradiated and irradiated thin films, respectively. These *I*–*V* curves were recorded by voltage cycling with increasing maximum amplitude, and the sequence of each voltage cycling is $0 \rightarrow -\text{max} \rightarrow 0 \rightarrow +\text{max} \rightarrow 0$. The maximum voltages for the nonirradiated and irradiated samples are 8 and 7.5 V, respectively. Both samples exhibit multilevel RS. They reveal one HRS and several LRSs, depending on the maximum positive bias. The current is increased after irradiation, retaining the rectifying *I*–*V* characteristic. By

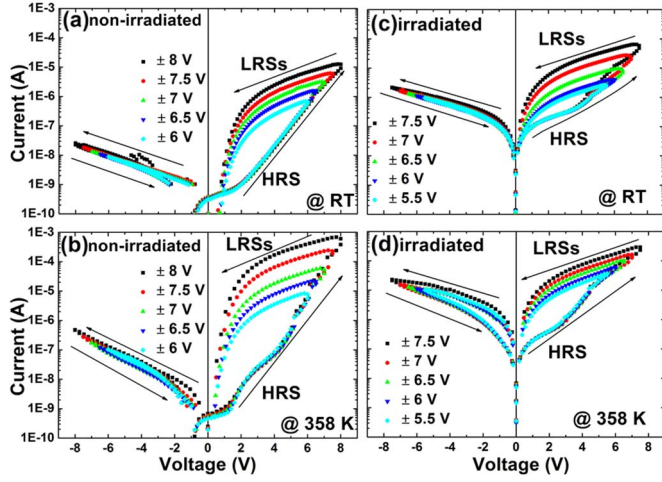


Fig. 1. I - V curves of (a) and (b) nonirradiated BFO thin films and of (c) and (d) Ar^+ irradiated BFO thin films at (a) RT and (b) and (d) 358 K.

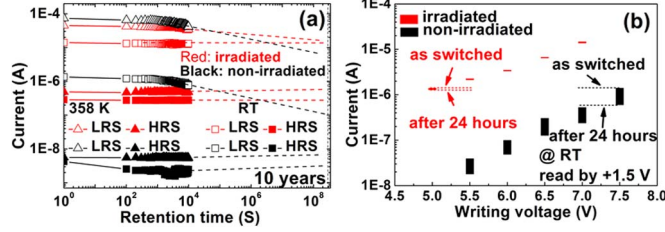


Fig. 2. (a) Retention test read by +1.5 V voltage pulses after switching at (squares) RT and (triangles) 358 K. (b) Currents versus writing voltages. The currents were measured directly after switching (top edge of the rectangles) and 24 h later (bottom edge of the rectangles).

increasing the temperature to 358 K, both thin films still exhibit multilevel RS characteristics, as shown in Fig. 1(b) and (d). The RS nonvolatility was examined by a retention test. Voltage pulses of ± 8 and ± 7.5 V were used to switch the nonirradiated and irradiated thin films, respectively. Pulses larger than $+5$ V set the thin films into one of the LRSs, and pulses smaller than -5 V reset them into the HRS. Subsequently, the resistance state was read out by a small voltage pulse of +1.5 V. As shown in Fig. 2(a), the nonirradiated BFO thin film exhibits fast degradation of the LRS within 10^4 s (black squares) at RT. This degradation is frequently found in the retention test of the as-grown BFO sample [8]. In contrast, the irradiated thin film shows an improved retention property (red squares). The extrapolated value of the ON/OFF ratio after ten years does not differ from the initial value after the first switching. The retention test was also carried out at 358 K. In that case, the LRS of the irradiated thin film also degrades (red empty triangles) but not as significantly as that of the nonirradiated film (black empty triangles).

The retention of multilevel RS at RT is shown in Fig. 2(b). Five LRSs have been obtained in both samples by different writing pulses. For the nonirradiated thin film, adjacent resistance states become indistinguishable after 24 h due to the degradation of the measured current. The overlapping of resistance states makes the device impractical for multilevel switching. In contrast, the current degradation is suppressed significantly in the irradiated thin film. No overlapping has been observed between the resistance windows, and all of the resistance states

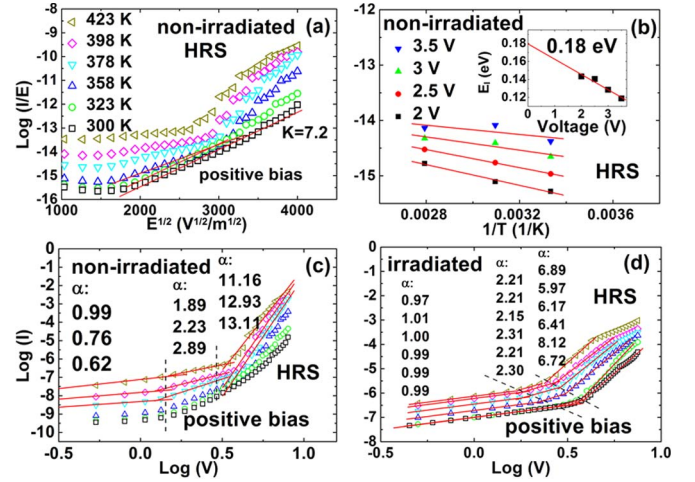


Fig. 3. (a) $\log (I/E)$ - $E^{1/2}$ plot (PF) and (b) Arrhenius plot of trap ionization energy E_I for the HRS of nonirradiated thin films. The inset in (b) shows the estimation of zero-bias trap ionization energy. $\log (I)$ - $\log (V)$ plots (SCLC) for (c) nonirradiated and (d) irradiated thin films, respectively.

can be still distinguished after 24 h. That indicates the improved retention property after irradiation.

Both the nonirradiated and irradiated thin films exhibit a rectifying behavior (see Fig. 1). The top Au/BFO interface establishes a Schottky contact due to the n-type conductivity of BFO [8]. When negative bias is applied to the Au top electrode, the I - V curves of the structures show much lower leakage currents without hysteresis. This is due to the current limitation by the high Schottky barrier. However, conductivity switching of BFO is revealed by the strong IV hysteresis under positive bias, and the LRSs of nonirradiated films tend to degrade. To understand the stabilization of LRSs by irradiation, the conduction mechanisms of the IV hysteresis under positive bias need to be clarified.

The HRS IV branches of the nonirradiated film show Poole-Frenkel (PF) conduction below 358 K and space-charge-limited conduction (SCLC) above 358 K, as confirmed by the linear fits in Fig. 3(a) and (c), respectively. The PF and SCLC mechanisms can be described as follows:

$$J = BE \exp - \left(\frac{E_I}{kT} - \frac{q}{kT} \sqrt{\frac{qE}{\pi \epsilon_0 K}} \right) \quad \text{PF} \quad (1)$$

$$J = \frac{9\mu\epsilon_0\epsilon_r E^2}{8d} \quad \text{SCLC.} \quad (2)$$

As shown in Fig. 3(a), a linear fit can be obtained for temperatures between RT and 358 K in a $\log(I/E)$ - $E^{1/2}$ scale, which reveals the PF conduction. The dielectric constant of $K \sim 7.2$ can be deduced from the slope of the curve. It is consistent with the value of 6.25 given in a previous report [11]. The zero-bias trap ionization energy E_I is estimated to be 0.18 eV [see Fig. 3(b)]. Above 358 K, the linear fits shown in Fig. 3(c) are obtained with three different slopes for each temperature. This behavior is typical for SCLC.

In the case of the irradiated BFO film, only SCLC occurs at the HRS [see Fig. 3(d)]. Over the whole temperature range from RT to 423 K, all IV curves can be fitted with reasonable slopes for SCLC. The SCLC is mainly induced by the high density of free charge carriers in the films, which are generated

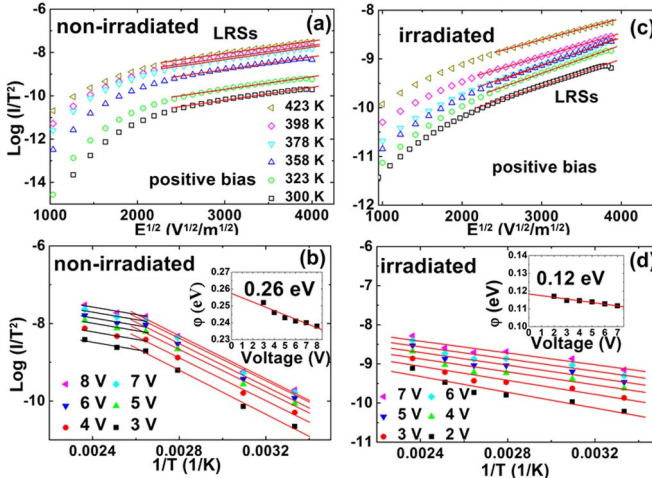


Fig. 4. $\log(I/T^2) - E^{1/2}$ plots under positive bias for the LRSs of (a) nonirradiated and (c) irradiated thin films. Arrhenius plots for the barrier height of the BFO/Pt interface for (b) nonirradiated and (d) irradiated thin films, respectively. The insets in (b) and (d) show the estimation of the zero-bias Schottky barrier height of the BFO/Pt interface (b) before and (d) after irradiation.

either by Ar^+ irradiation in the irradiated samples or by thermal ionization in the nonirradiated sample at elevated temperatures.

Different from the bulk-limited conduction at HRS, interface-limited Schottky emission (SE) dominates the LRS conduction, as shown in Fig. 4(a) and (c). SE conduction is described by the formula

$$J = A^* T^2 \exp - \left(\frac{\varphi_b}{kT} - \frac{q}{kT} \sqrt{\frac{qE}{4\pi\varepsilon_0 K}} \right) \quad \text{SE.} \quad (3)$$

In contrast to the rectifying Au/BFO interface, the BFO/Pt/Ti interface is nonrectifying, which may be induced by the interdiffusion of Ti to the BFO/Pt interface. A small barrier exists causing SE conduction for LRS under positive bias. The barrier heights are deduced to be 0.26 eV (nonirradiated) and 0.12 eV (irradiated) from the Arrhenius plots shown in Fig. 4(b) and (d), respectively. Note that the Arrhenius plot of the nonirradiated sample shows nonlinearity at higher temperatures, which also can be fitted with a smaller barrier height value [see Fig. 4(b)]. This is due to the inhomogeneity of the interface [12], [13]. Further investigation is needed to determine the barrier height in this sample with higher accuracy. Low barriers allow for electron injection from the Pt/Ti electrode into the BFO film under positive bias. This reduces the resistance of the bulk BFO layer. Therefore, the leakage current at LRSs is not bulk limited and mainly controlled by the BFO/Pt interface.

According to this mechanism, filling of electron trapping sites under positive bias switches the BFO thin film to the LRS. The LRS retention is substantially influenced by the stability of the trapped electrons within the trapping sites [14].

The trapping sites in the BFO film include grain boundaries, ions, OVs, and so on. When Ar^+ ions impinge on the BFO film surface, the light element oxygen is preferentially sputtered from the materials surface, which results in the formation of OVs in the near-surface region. Due to the concentration gradient of OVs, the OVs diffuse [15], [16] into the BFO bulk

under the irradiation conditions. The creation and redistribution of OVs reduce the randomness of unstable defects in the BFO thin film and contribute to the stabilization of interface-related RS. Due to the significant increase in switching current density and Joule heating, degradation of endurance may occur in the irradiated sample. However, this degradation is expected to be suppressed after downscaling of the device and reduction of the reading bias.

In summary, nonvolatile multilevel RS was observed in an Au/BFO/Pt capacitor structure. The retention of the LRSs was improved in a controllable manner by Ar^+ ion irradiation. The conduction mechanisms of the structures are discussed. Stabilization of the LRSs is attributed to the reduced randomness of the defect states induced by manipulation of the OV concentration via irradiation. This letter shows that low-energy ion irradiation is an efficient tool for tuning of the RS properties of interface-related RS.

REFERENCES

- [1] A. Sawa, "Resistive switching in transition metal oxides," *Mater. Today*, vol. 11, no. 6, pp. 28–36, Jun. 2008.
- [2] R. Waser and M. Aono, "Nanoionics-based resistive switching memories," *Nat. Mater.*, vol. 6, no. 11, pp. 833–840, Nov. 2007.
- [3] D. B. Strukov, G. S. Snider, D. R. Stewart, and R. S. Williams, "The missing memristor found," *Nature*, vol. 453, no. 7191, pp. 80–83, May 2008.
- [4] C. Blee, B. S. Kang, A. Benayad, M. J. Lee, S.-E. Ahn, K. H. Kim, G. Stefanovich, Y. Park, and I. K. Yoo, "Effects of metal electrodes on the resistive memory switching property of NiO thin films," *Appl. Phys. Lett.*, vol. 93, no. 4, pp. 042115-1–042115-3, Aug. 2008.
- [5] C. Joonhyuk, J. Song, K. Jung, Y. Kim, H. Im, W. Jung, H. Kim, Y. H. Do, J. S. Kwak, and J. Hong, "Bipolar resistance switching characteristics in a thin Ti-Ni-O compound film," *Nanotechnology*, vol. 20, no. 17, p. 175704, Apr. 2009.
- [6] C. Moreno, C. Munuera, S. Valencia, F. Kronast, X. Obradors, and C. Ocal, "Reversible resistive switching and multilevel recording in La_{0.7}Sr_{0.3}MnO₃ thin films for low cost nonvolatile memories," *Nano Lett.*, vol. 10, no. 10, pp. 3828–3835, Oct. 2010.
- [7] S. D. Ha and S. Ramanathan, "Adaptive oxide electronics: A review," *J. Appl. Phys.*, vol. 110, no. 7, pp. 071101-1–071101-20, Oct. 2011.
- [8] Y. Shuai, S. Zhou, D. Bürger, M. Helm, and H. Schmidt, "Nonvolatile bipolar resistive switching in Au/ BiFeO₃/Pt," *J. Appl. Phys.*, vol. 109, no. 12, pp. 124117-1–124117-4, Jun. 2011.
- [9] S. Hirose, A. Nakayama, H. Niimi, K. Kageyama, and H. Takagi, "Improvement in resistance switching and retention properties of Pt/TiO₂ Schottky junction devices," *J. Electrochem. Soc.*, vol. 158, no. 3, pp. H261–H266, 2011.
- [10] D. W. Reagor and V. Y. Butko, "Highly conductive nanolayers on strontium titanate produced by preferential ion-beam etching," *Nat. Mater.*, vol. 4, no. 8, pp. 593–596, Aug. 2005.
- [11] S. Iakovlev, C. H. Solterbeck, M. Kuhnke, and M. Es-Souni, "Multi-ferroic BiFeO₃ thin films processed via chemical solution deposition: Structural and electrical characterization," *J. Appl. Phys.*, vol. 97, no. 9, pp. 094901-1–094901-6, May 2005.
- [12] R. T. Tung, "Electron transport of inhomogeneous Schottky barriers," *Appl. Phys. Lett.*, vol. 58, no. 24, pp. 2821–2823, Jun. 1991.
- [13] J. H. Werner and H. H. Guttler, "Barrier inhomogeneities at Schottky contacts," *J. Appl. Phys.*, vol. 69, no. 3, pp. 1522–1533, Feb. 1991.
- [14] C. An, S. Haddad, and W. Yi-Ching, "A temperature-accelerated method to evaluate data retention of resistive switching nonvolatile memory," *IEEE Electron Device Lett.*, vol. 29, no. 1, pp. 38–40, Jan. 2008.
- [15] C.-H. Yang, J. Seidel, S. Y. Kim, P. B. Rossen, P. Yu, M. Gajek, Y. H. Chu, L. W. Martin, M. B. Holcomb, Q. He, P. Maksymovych, N. Balke, S. V. Kalinin, A. P. Baddorf, S. R. Basu, M. L. Scullin, and R. Ramesh, "Electric modulation of conduction in multiferroic Ca-doped BiFeO₃ films," *Nat. Mater.*, vol. 8, no. 6, pp. 485–493, 2009.
- [16] H. Gross, N. Bansal, Y. S. Kim, and S. Oh, "In situ study of emerging metallicity on ion-bombarded SrTiO₃ surface," *J. Appl. Phys.*, vol. 110, no. 7, pp. 073704-1–073704-6, Oct. 2011.